water

MDPI

Article

Stormwater Tree Pits for Decentralized Retention of Heavy Rainfall

Nils Siering * and Helmut Grüning

Faculty of Energy Building Services Environmental Engineering, FH Münster University of Applied Sciences, Stegerwaldstraße 39, 48565 Steinfurt, Germany; gruening@fh-muenster.de
* Correspondence: nilssiering@fh-muenster.de; Tel.: +49-2551-962-501

Abstract: Stormwater tree pits with storage elements enable the irrigation of urban trees and can potentially act as decentralized rainwater retention basins. This paper mainly focuses on analyzing this potential. Field tests were conducted to investigate the irrigation behavior and the storage effect of a storm water tree pit system using Perl hoses as irrigation elements over a period of two years. The rainfall, storage volumes, and soil moisture within the employed planting pit were measured. With the help of system modeling, the retention ability of the storm water tree pit system was analyzed. The available storage volume was sufficient to irrigate trees for several days. During the measurement period, about 15% of the inflowing rainwater was fed to the root zone of the tree. With practical storage volumes of 200 to 300 m^3/ha, a remarkable amount of water from heavy rainfall could be completely stored, thus significantly reducing the risk of flooding. The retention effect and irrigation behavior largely depend on the soil conditions and the technical possibilities of the equipment supplying the root area (in this case, Perl hoses). Further investigations are required to determine the influence on the growth conditions of trees and optimize of the system for discharge into the root zone.

Keywords: stormwater tree pits; decentralized storm water retention system; flood prevention; soil moisture content; irrigation elements; Perl hoses

Citation: Siering, N.; Grüning, H. Stormwater Tree Pits for Decentralized Retention of Heavy Rainfall. *Water* **2023**, *15*, 2987. https://doi.org/10.3390/w15162987

Academic Editors: Enedir Ghisi and Brigitte Helmreich

Received: 30 June 2023
Revised: 13 August 2023
Accepted: 15 August 2023
Published: 18 August 2023

1. Introduction

Pronounced dry and hot spells and flooding caused by heavy rainfall due to climatic changes impair living conditions in urban areas. Water-conscious urban development measures are designed to induce cooling effects and reduce flooding risks. These measures also include stormwater tree pits, which are elements of blue–green infrastructure measures. Trees influence the urban climate through providing shade and evaporation and thus reduce the urban heat island effect [1]. However, the conditions of trees in urban areas are characterized by a lack of space and, during the spring and summer months, water stress as well [2]. In this regard, retention systems at tree sites can have a significant impact by, ideally, allowing both runoff from heavy rains to be locally stored and trees to be irrigated. Attempts have already been made to direct surface runoff into the root zones of urban trees through stormwater tree pits (e.g., the Stockholm Model) [3]. It has been shown that if optimal drainage is ensured, trees receiving stormwater runoff can present double the growth of conventionally planted street trees [4]. Though some articles report negative effects [5], more articles report positive effects [2,6–8]. Systems and concepts vary, ranging from hydrologically optimized tree sites to tree infiltration trenches with storage spaces acting as stormwater storage, like decentralized stormwater detention basins, in order to store runoff and attenuate peak flows. On the other hand, the storage spaces serve as irrigation elements. Some of the relevant challenges and divergent sub-objectives are as follows.

- A full reservoir ensures a maximum irrigation period but not the attenuation of the runoff peak.
- Excessively intensive irrigation inhibits root development and, in extreme cases, poses a risk of waterlogging.
- Water reaches the roots of young trees when irrigation is applied near the surface, but the storage potential is then limited to the root zone.
- Pollutant discharge, such as deicing salts and heavy metals that have leached from roof surfaces via rainfall, can negatively affect trees and thus should be prevented form entering the root zone untreated.

The issues surrounding the design, construction, and operation of stormwater tree pits are complex and far from settled. In addition to these challenges, there are still pending issues regarding stormwater tree pits:

- Pollutant entry and retention in the soil or substrate as well as the potentially necessary pretreatment of inflowing runoff.
- Root expansion in stormwater tree pits.
- Suitable tree choice in terms of alternating dry and wet periods.
- The extent of waterlogging periods.

The aim of this paper is to analyze the potential of storm water tree pits with storage elements to act as decentralized storm water retention basins. The possibility of flood prevention is considered, and it is shown which heavy rains can be completely or at least partially retained over the course of a year until emergency discharge into a sewer system or a surface water body occurs. The usage of Perl hoses as passive irrigation limiters to prevent excessive premature exfiltration beyond the trees' need was also tested. The balancing of the runoff and the storage behavior is achieved via model simulation and measurements taken in the years from 2021 to 2023.

2. Materials and Methods

2.1. Study Site

Within the scope of the investigations, the integration of stormwater tree pits into a traffic area and the effects of the systems were examined at different locations in Nottuln (North Rhine, Westphalia). The results presented herein correspond to an area on the company premises of Humberg GmbH (51°54′45″ N, 7°24′2″ E). There, the system was investigated together with two reference trees without stormwater tree pits. The site has a groundwater flow distance of 8.94 m and an infiltration rate of 4.37×10^{-6} m/s. The climate is classified as cfb, a temperate oceanic climate, according to the Koppen–Geiger climate classification, with an annual mean precipitation of 865 mm and a mean air temperature of 10.4 °C (1991–2021) [9].

2.2. Design of ALVEUS Stormwater Tree Pit and Reference Tree Pits

An overview of the ALVEUS system (proper name given by the manufacturer) (Sys) is given in Figure 1. The system is composed of galvanized steel with the following dimensions: 2000 mm × 3000 mm × 1619 mm (w × l × h). It consists of three reservoir levels: the reservoir in the irrigation grating system (1), the irrigation reservoir (2; the upper reservoir), and the infiltration or retention reservoir (3; the lower reservoir). The upper and lower reservoir levels consist of two connected, opposite reservoirs, respectively. Water from the surrounding surface (7) flows into the irrigation grating system with a maximum capacity of 100 L. Small outlets are located at the lowest points, i.e., near the tree trunk (10). If the water level in the irrigation grating reaches the maximum capacity, the excess water flows into the irrigation reservoir (2) via an overflow edge (8), which has a maximum capacity of 258 L per side. Additional runoff, e.g., from roofs or surfaces located further away from the system, flows directly into the irrigation reservoir (6). In this study, 300 m^2 of the factory building (with a discharge coefficient $\Psi = 0.95$) were connected to the system. Four ball valves were located on each side of the irrigation reservoir facing the root

ball, which was equipped with Perl hoses (4; depicted as a mesh) that gradually release water into the root zone (10). The balls valves can be closed in the winter to prevent water contaminated with deicing salts from entering the root zone. If the irrigation reservoir also reaches its capacity, excess water flows into the infiltration reservoir (3), which also occurs via an overflow edge (8). The maximum capacity of the infiltration reservoir is 890 L per side. From the reservoir, the water can infiltrate the adjacent soil via the openings in the bottom of the reservoir (11). These openings can be sealed with a rubber mat, and a pump can be installed to store the water and use it for irrigation for longer durations during dry periods (9). If the infiltration reservoir also reaches capacity, excess water will be discharged from the system via an emergency overflow, which is either connected to the rainwater sewage system or a nearby body of water (12). To ensure a supply of oxygen and the discharge of carbon dioxide, a ventilation element is located near the bottom of the root zone (5).

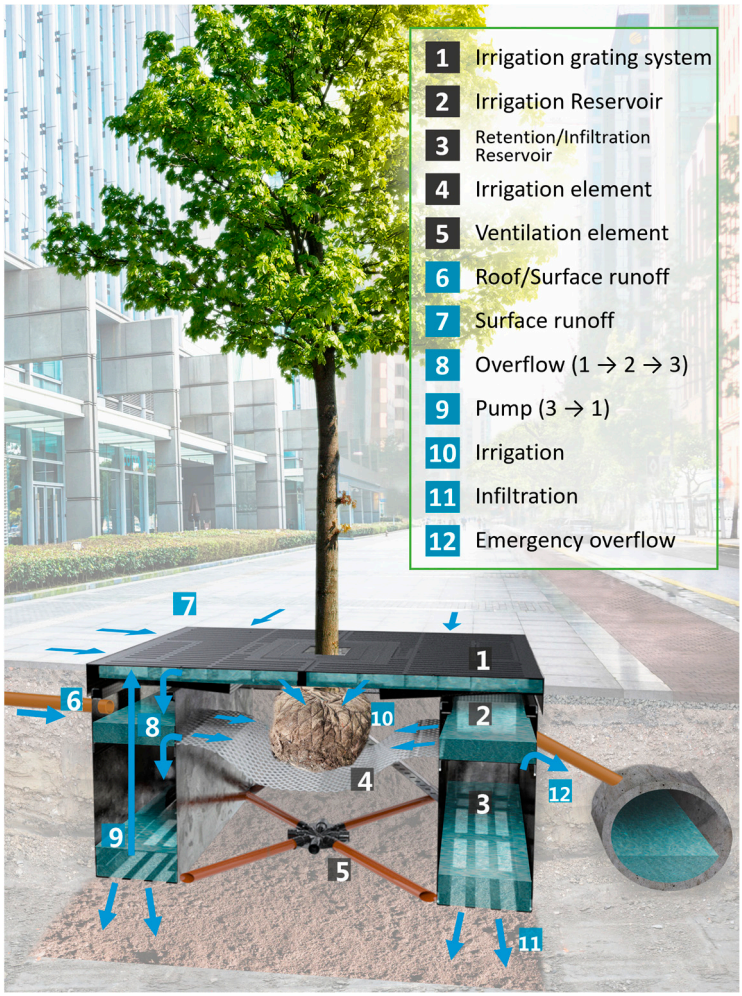

Figure 1. Overview of the stormwater tree pit system ALVEUS (water flow paths represented by blue arrows).

In order to examine the effects and possible benefits of the stormwater tree pit system, two reference tree pits were also monitored. The first reference tree pit (Ref) was constructed such that it had an unprotected surface area. The second reference tree (Prg) was equipped with a protective grid, which was also manufactured by the Humberg GmbH.

All three tree locations were supplemented with the vegetation substrate Vulcatree L 0–32 (VulkaTec Riebensahm GmbH, Andernach, Germany), which was used according to the manufacturer's guidelines. The substrate possessed a pH value of 7.0 to 7.5, a salinity content of 100 to 500 mg/kg, a maximum water-retaining capacity in the range of 20 to

25 Vol.-%, and an infiltration rate in the range of 5×10^{-6} to 3×10^{-4} m/s, according to the manufacturer's specifications.

The dimensions of the planting pits can be found in Figure 2. The species "liquidamber straciflua" was planted in all tree pits.

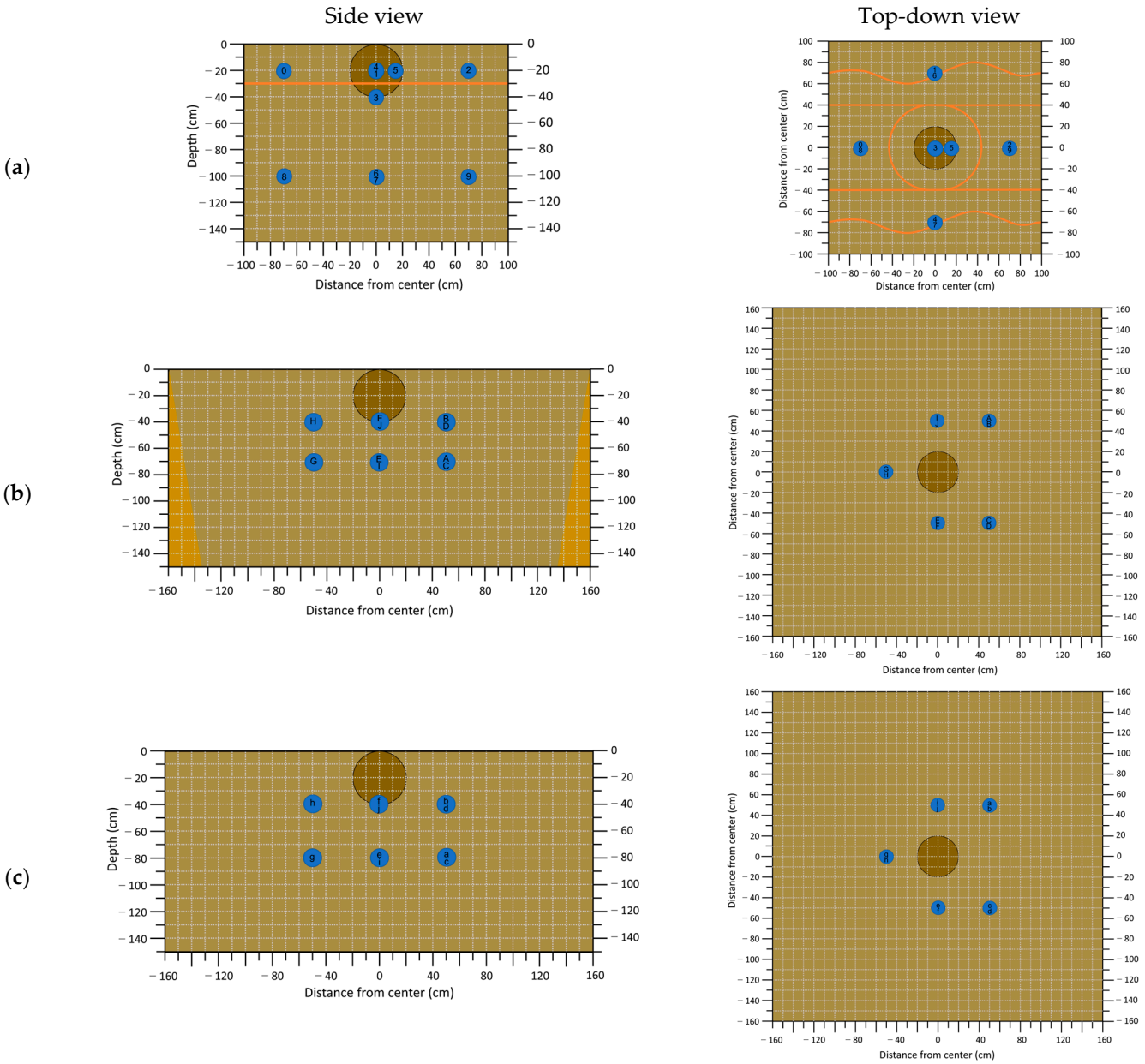

Figure 2. Layouts of the tree pits with volumetric water content probes (blue), root balls (dark brown), vegetative substrate (light brown), natural soil (orange-brown), and Perl hoses (orange): (**a**) ALVEUS system (Sys), probes 0–9; (**b**) reference tree (Ref), probes A–J; (**c**) protective grate (Prg), probes a–j.

2.3. Water Level Measurements and Soil Moisture Content

Water level probes (NTB-130215, KOBOLD Messring GmbH, Hofheim am Taunus, Germany) were installed at the irrigation and infiltration reservoir levels. Additionally, volumetric water content probes (VWC; SMT100 SDI-12, TRUEBNER GmbH, Ludwigshafen, Germany) were installed at varying depths (10 probes per tree pit) to monitor the effects of irrigation on the water balance in the tree pits. The layout of the tree pits can be seen in Figure 2.

In order to convert the measurement data obtained from the soil water content probes, the water retention characteristics of the vegetation substrate were analyzed as water content at characteristic pressure levels of pH 1.8, 2.5, and 4.2 as a percentage of weight using a pressure plate apparatus. The relative extractable soil water content (REW) was calculated using the formula provided in [10]:

$$\text{REW } (\%) = 100 \cdot ((\text{VWC}_{\text{actual}} - \text{VWC}_{\text{PWP}}) \cdot (\text{VWC}_{\text{FC}} - \text{VWC}_{\text{PWP}})^{-1}) \quad (1)$$

where VWC_{PWP} is the water content at the permanent wilting point (PWP, pF = 1.8) and VWC_{FC} is the water content at field capacity (pF = 4.2).

2.4. Meteorological Data

Rainfall at the experimental site was recorded using a tipping bucket rain gauge (Kalyx-RG, Campbell Scientific Europe, Loughborough, UK). Data from the regionalized statistical heavy rain analysis (KOSTRA-DWD) taken from the German weather service (DWD) site were used to determine the storable heavy rain events in relation to the connected impervious area [11].

2.5. Water Distribution Model

The water distribution model of the ALVEUS system was constructed by implementing simplifications and making assumptions to account for data that could not be recorded at the study site. These simplifications and assumptions are as follows:

- Perl hoses and infiltration: the exfiltration rate of the Perl hoses and the rate of infiltration into the lower soil are majorly influenced by the current water level in the respective reservoir.
- Perl hoses: the exfiltration rate of the Perl hoses is influenced by the growing season (roughly Mai–September in Germany) [12]
- Evaporation: the evaporation of water in the reservoirs is negligible.
- Irrigation grating system: the reservoir in the irrigation grating system was excluded from the model.

The only dynamic input for the model was precipitation. Volumetric losses due to the wetting of the surface and surface depressions were initially considered but then discarded when their influence was found to be negligible. The corresponding Equations (3)–(10) were formulated for the model (symbol explanations given in Table 1, Figure 3 shows a flow diagram for easier understanding):

Connected impermeable surface:

$$A_{\text{imp.}} = A_E \cdot \psi \quad (2)$$

Exfiltration through the Perl hoses:

$$q_{\text{Perl,max}} = \begin{cases} q_{\text{Perl,max,gs}}, & \text{for } 5 < m < 9 \\ q_{\text{Perl,max,ngs}}, & \text{for } m < 5 \vee m > 9 \\ q_{\text{Perl,max,gs}} \cdot \frac{d}{31} + q_{\text{Perl,max,ngs}} \cdot \frac{31-d}{31}, & \text{for } m = 5 \\ q_{\text{Perl,max,gs}} \cdot \frac{31-d}{31} + q_{\text{Perl,max,ngs}} \cdot \frac{d}{31}, & \text{for } m = 9 \end{cases} \quad (3)$$

$$q_{\text{Perl}} = \begin{cases} q_{\text{Perl,max}} \cdot \left(p_{\text{stat,UR}} + p_{\text{dyn,UR}} \cdot \frac{h_{\text{UR}}(t-1) - O_{\text{UR}}}{h_{\text{UR,max}} - O_{\text{UR}}} \right), & \text{for } h_{\text{UR}}(t-1) > O_{\text{UR}} \\ q_{\text{Perl,max}} \cdot p_{\text{stat, UR}}, & \text{for } h_{\text{UR}}(t-1) \leq O_{\text{UR}} \end{cases} \quad (4)$$

Irrigation reservoir:

$$h_{\text{UR,th}}(t) = h_{\text{UR}}(t-1) + \frac{r(t) \cdot A_{\text{imp.}}}{A_{\text{UR}}} - q_{\text{Perl}} \cdot \triangle t \quad (5)$$

$$h_{UR}(t) = \begin{cases} h_{UR,th}(t), & \text{for } h_{UR,max} > h_{UR,th}(t) > 0 \\ h_{UR,max}, & \text{for } h_{UR,max} \geq h_{UR,th}(t) \\ 0, & \text{for } h_{UR,th}(t) \leq 0 \end{cases} \quad (6)$$

Infiltration:

$$q_{inf} = \begin{cases} q_{inf,max} \cdot \left(p_{stat,LR} + p_{dyn,LR} \cdot \frac{h_{LR}(t-1) - O_{LR}}{h_{LR,max} - O_{LR}} \right), & \text{for } h_{LR}(t-1) > O_{LR} \\ q_{inf,max} \cdot p_{stat,LR}, & \text{for } h_{LR}(t-1) \leq O_{LR} \end{cases} \quad (7)$$

Infiltration Reservoir:

$$h_{LR,th}(t) = \begin{cases} h_{LR}(t-1) + \frac{(h_{UR}(t) - h_{UR,max}) \cdot A_{UR}}{A_{LR}} - q_{inf} \cdot \triangle t, & \text{for } h_{UR,th}(t) > h_{UR,max} \\ h_{LR}(t-1) - q_{inf} \cdot \triangle t, & \text{for } h_{UR,th}(t) \leq h_{UR,max} \end{cases} \quad (8)$$

$$h_{LR}(t) = \begin{cases} h_{LR,th}(t), & \text{for } h_{UR,max} > h_{UR,th}(t) > 0 \\ h_{LR,max}, & \text{for } h_{LR,th}(t) \geq h_{LR,max} \\ 0, & \text{for } h_{LR,th}(t) \leq 0 \end{cases} \quad (9)$$

Emergency overflow:

$$V_E(t) = \begin{cases} (h_{LR,th}(t) - h_{LR,max}) \cdot A_{LR}, & \text{for } h_{LR,th}(t) \geq h_{LR,max} \\ 0, & \text{for } h_{LR,th}(t) \leq h_{LR,max} \end{cases} \quad (10)$$

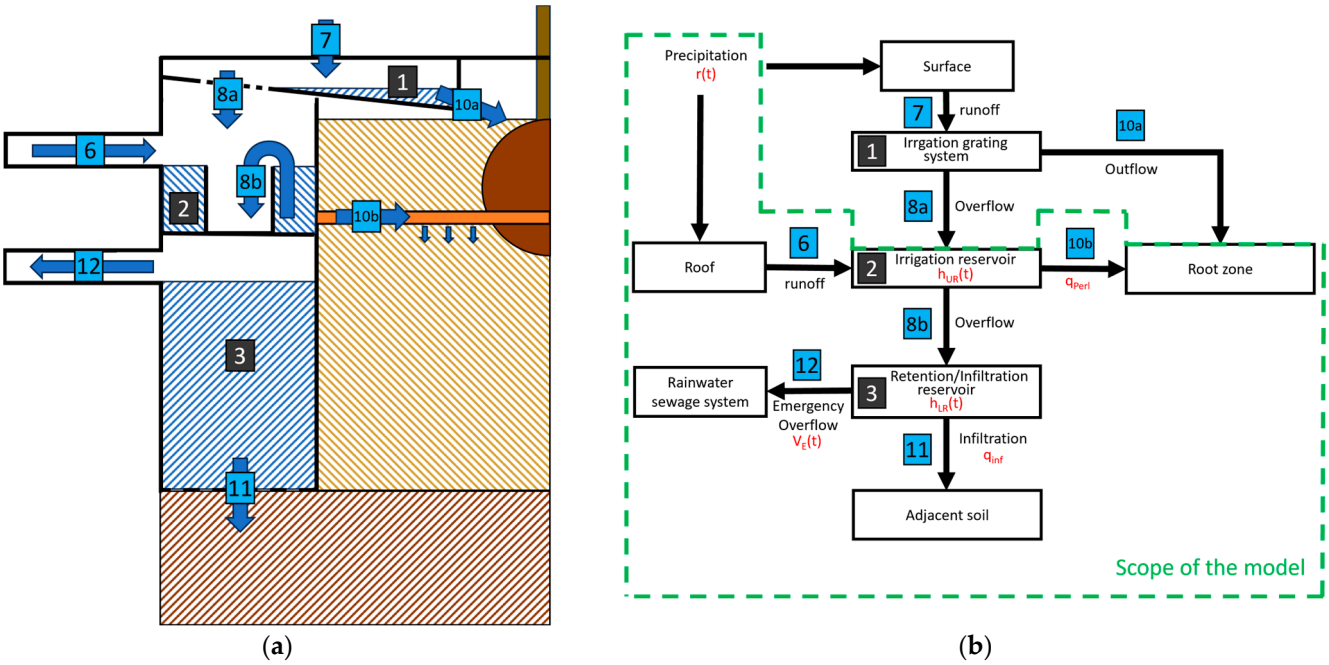

Figure 3. Side by side comparison of a schematic overview and a flow diagram of the tree pit system. (**a**) Schematic overview of the tree pit system (halved) (blue—maximum water levels of the corresponding reservoirs); (**b**) flow diagram of the system and the scope of the model (corresponding equation symbols marked in red).

Table 1. Symbol explanations and values of static symbols.

Symbol	Title 2	Value	Unit
$A_{imp.}$	Impervious connected area	285	m^2
A_E	Connected area	300	m^2
A_{LR}	Base area of the infiltration reservoir (lower reservoir)	2.30146	m^2
A_{UR}	Base area of the irrigation reservoir (upper reservoir)	1.141	m^2
d	Current day of date t	-	-
$h_{LR}(t)$	Water level of the infiltration reservoir on date t	-	mm
$h_{LR}(t-1)$	Water level of the infiltration reservoir on date $t-1$	-	mm
$h_{LR,max}$	Maximum water level of the infiltration reservoir	1050	mm
$h_{LR,th}(t)$	Theoretical water level of the infiltration reservoir on date t	-	mm
$h_{UR}(t)$	Water level of the irrigation reservoir on date t	-	mm
$h_{UR}(t-1)$	Water level of the irrigation reservoir on date $t-1$	-	mm
$h_{UR,max}$	Maximum water level of the irrigation reservoir	288	mm
$h_{UR,th}(t)$	Theoretical water level of the irrigation reservoir on date t	-	mm
m	Current month of date t	-	-
$p_{stat,LR}$	Static part of the infiltration rate of the lower soil	0.1	-
$p_{stat,UR}$	Static part of the exfiltration rate of the Perl hoses	0.3	-
$p_{dyn,LR}$	Dynamic part of the infiltration rate of the lower soil	0.9	-
$p_{dyn,UR}$	Dynamic part of the exfiltration rate of the Perl hoses	0.7	-
$q_{inf,max}$	Maximum infiltration rate in the lower soil	2	$mm \times min^{-1}$
$q_{Perl,max}$	Maximum exfiltration rate of the Perl hoses	-	$mm \times min^{-1}$
$q_{Perl,max,gs}$	Maximum exfiltration rate of the Perl hoses during growing season	0.014	$mm \times min^{-1}$
$q_{Perl,max,ngs}$	Maximum exfiltration rate of the Perl hoses outside of the growing season	0.6	$mm \times min^{-1}$
r(t)	Rainfall that occurred in the period between $t-1$ and t	-	mm
t	Date	-	-
Δt	Time resolution of the simulation/measurements	5	min
$V_E(t)$	Emergency overflow volume on date t	-	m^3

The model was then transferred into a python program (V. 3.9.12), where the static variables were adjusted using the root mean square error (RMSE) and the mean absolute error (MAE) to achieve the best possible model accuracy while attempting to limit the extent of overfitting of the model to the data used for calibration (the measurement data concerning the period from 29 April 2021 to 30 November 2022).

2.6. Retainable Heavy Rain Events

Regional statistical heavy rain events (see Section 2.4) were used as an input for the water distribution model to determine the heavy rain events that can be retained in the system relative to the connected impervious area. If no emergency discharge was recorded ($\sum V_E = 0$), the heavy rain event was classified as "retainable". This analysis was carried out for two different initial situations: a situation where the system was assumed to be empty ($h_{UR}(t = 0) = 0$ and $h_{LR}(t = 0) = 0$) and a situation where median measured water levels were used ($h_{UR}(t = h_{UR,med})$ and $h_{LR}(t = h_{LR,med})$). Furthermore, the analysis was separated into periods during and outside of the growing season (roughly corresponding to May–September) because of the different exfiltration rates shown through the observation and modeling approach.

3. Results

3.1. Water Level Measurements and Soil Moisture Content

The recorded water levels in the irrigation and infiltration reservoirs can be seen in Figures 4 and 5. The data present a clear difference between the exfiltration rates of the Perl hoses during and outside of the growing season (roughly May–September), while they also reveal wide variability in the exfiltration range during the growing season, ranging from 0.7 to 23.3 L/h. Seven occurrences of insufficient emergency discharge, where the water levels in the irrigation and infiltration reservoirs exceeded 288 mm and 1050 mm,

respectively, were observed in the study period. Long periods of empty irrigation reservoirs were observed in June 2021 and in July and August 2022. A period in which the water levels did not approach zero between rain events in the infiltration reservoir was observed in May and June 2022, when backwater possibly occurred. Throughout the study, around 13 to 15% of the inflowing water was transferred to the root zone, resulting in about 17 to 22 m^3 of additional irrigation per year. The amount of emergency overflow amounted to 8 to 10% of the inflowing water, thus a reduction of runoff by 90 to 92% was achieved.

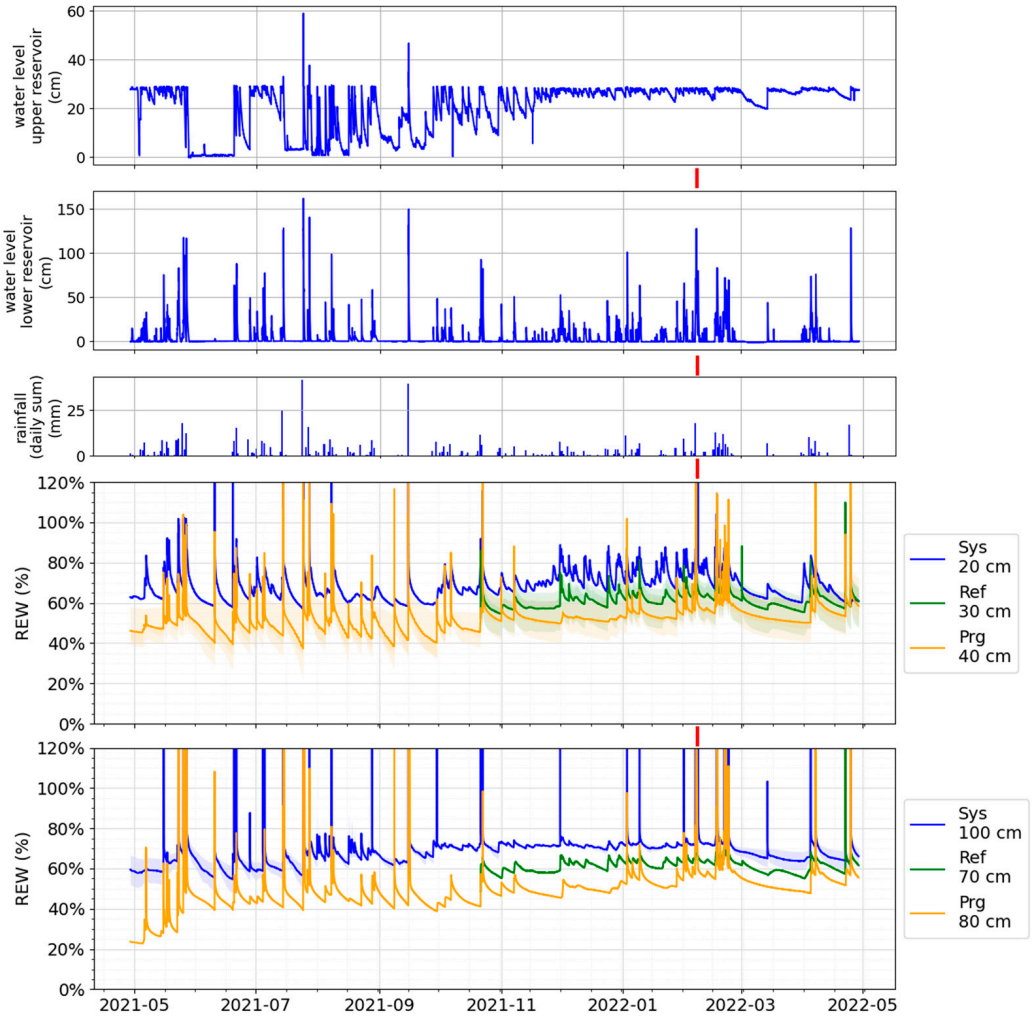

Figure 4. Measured water levels, precipitation levels, and relative extractable water (REW %) at various depths during the first year of observation (29 April 2021–28 April 2022). Bold lines represent the mean of all representative probes, while shaded areas indicate the range of individual representative probes. Outside influences are indicated as follows: red—flooding experiment.

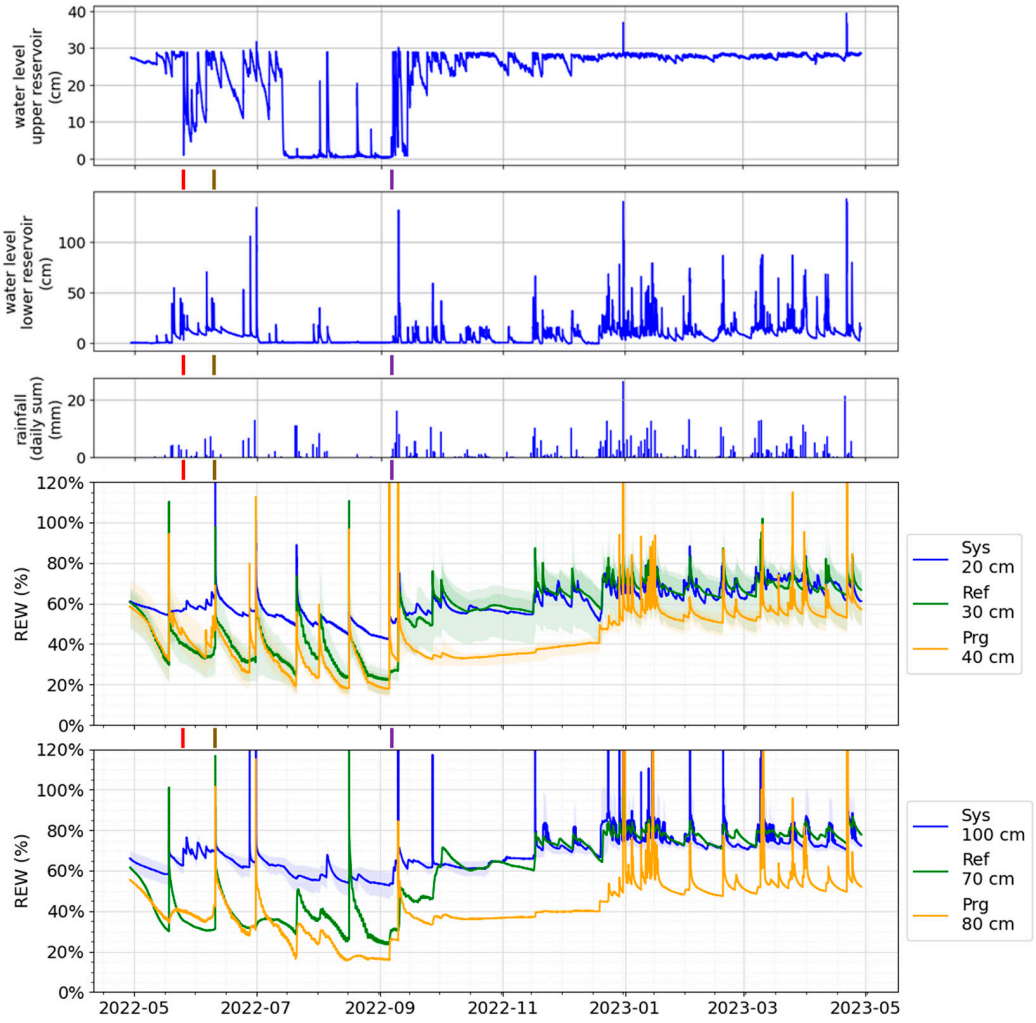

Figure 5. Measured water levels, precipitation levels, and relative extractable water (REW %) at various depths during the second year of observation (29 April 2022–28 April 2023). Bold lines represent the mean of all representative probes, while shaded areas indicate the range of individual representative probes. Outside influences are indicated as follows: red—rinsing of Perl hoses, brown—temporary sealing of inlets to the system for testing purposes, and purple—external watering of all trees.

Figure 6 shows the distribution of the measured water levels at both reservoir levels, where both reservoirs' datasets are also separated into periods during and outside of the growing season. The data from the lower infiltration reservoir level show little variance between water levels during and outside of the growing season and low median water levels in general, ranging from 0.412 cm during the growing season to 2.753 cm outside of the growing season. In contrast, the irrigation reservoir presents higher variability between seasons, with a median water level of 14.54 cm during the growing season and 27.44 cm outside of the growing season.

During the study, one soil water content probe failed. Additionally, due to problems with the data transfer process, no data are available for Ref for the first 6 months of the study. The soil water retention characteristic analysis delivered the following results regarding soil moisture content: 24.5 Vol.-% at pF = 1.8, 20.9 Vol.-% at pF = 2.5, and 11.0 Vol.-% at pF = 4.2 (n = 3, respectively). However, these determined values were incompatible with the soil moisture content measured on site and the measured tree growth because the REW would have, for the most part, been in the range of 0 to 40% (drought stress) [13–15] and often even below 0% for Prg. This can be explained by the poor connection of the coarse-grained vegetation substrate to the ceramic plates used in the determination method, which are

mostly used for more fine-grained, natural soils. Thus, for further analysis, a soil moisture content of 3.0 Vol.-% at PWP (pF = 4.2) was assumed. In addition, the individual soil moisture content probes showed a wide range of values, even in similar circumstances, such as one to three days after heavy rain events outside of the growing season, when soil moisture content can be assumed to be at field capacity (pF = 1.8). This can be explained by the ununiform installation of the probes caused by the coarse-grained composition of the vegetation substrate. Nevertheless, to ensure uniform conditions in the comparison, probes that measured values outside of the median value plus the manufacturer's given range of fluctuation (±3 Vol.-%) under field capacity conditions were excluded (~50% of probes). The adjusted soil moisture content data are also shown in Figures 4 and 5.

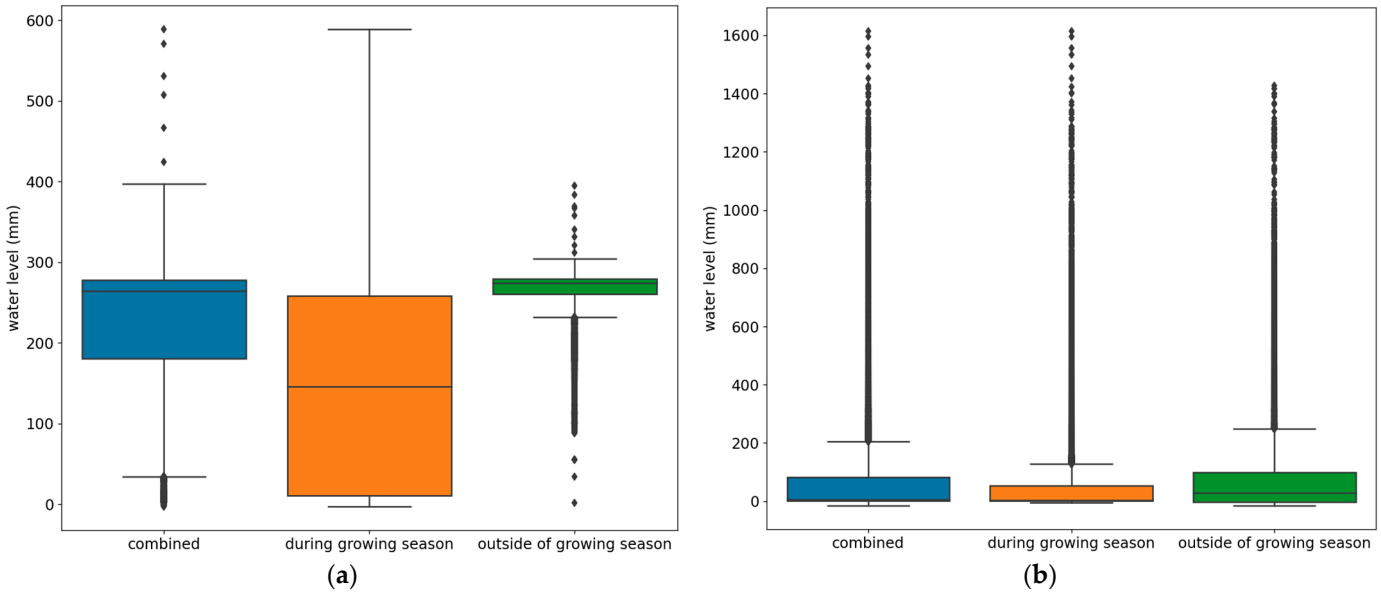

Figure 6. Measured water levels during the first and second years of observation (29 April 2021–28 April 2023) presented as boxplots and divided by growing season. (**a**) Irrigation reservoir; (**b**) infiltration reservoir.

As can be seen in Figures 4 and 5, the highest soil moisture content was primarily achieved by Sys, with Ref a few percentage points below this level for the first year of the study. Prg presented the lowest soil moisture content for the most part. During the growing season of the second year (May–September 2022), a depletion of the soil water balance was observed regarding Ref and Prg, while only a minor depletion was observed with respect to Sys. This can either be explained by the irrigation system working as intended or by the soil water probes being located further away from the root ball and the roots not having reached the influence area of the probes. The second explanation seems more likely since even during the long period of an empty irrigation reservoir in the second growing season (July–August 2022), no real sign of soil water balance depletion could be observed.

After the second growing season, the REW at Ref reached values similar to those of Sys for the rest of the studied year. Prg, however, showed no or insignificant signs of the soil water content reaching values similar to those observed before the growing season for the first months and only reached such values during the start of 2023; even then, they were still considerably lower than those observed for Sys and Ref.

The raw data files can be found in the supplementary materials: water levels (Tables S1 and S2); soil moisture content (Tables S3 and S4); precipitation (Tables S5 and S6).

3.2. Model Accuracy

The determined optimal static variable values are shown in Table 1. A visual comparison of model-predicted water levels with measured water levels can be seen in Figures 7 and 8.

RMSE values of 9.19 cm and 6.14 cm were achieved for the irrigation and infiltration reservoirs, respectively. Accordingly, MAE values of 5.69 cm and 2.89 cm were determined. It can be seen that the water levels observed outside of the growing season matched well. For the growing season, however, the model showed far greater differences between the simulated and measured values.

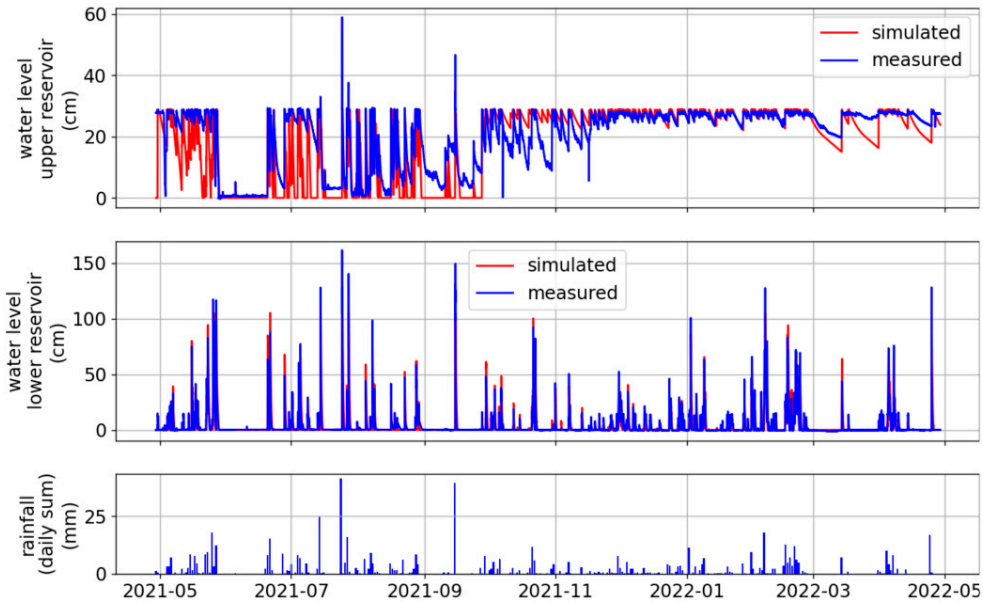

Figure 7. Comparison of model-predicted water levels with measured water levels during the first year of observation (29 April 2021–28 April 2022).

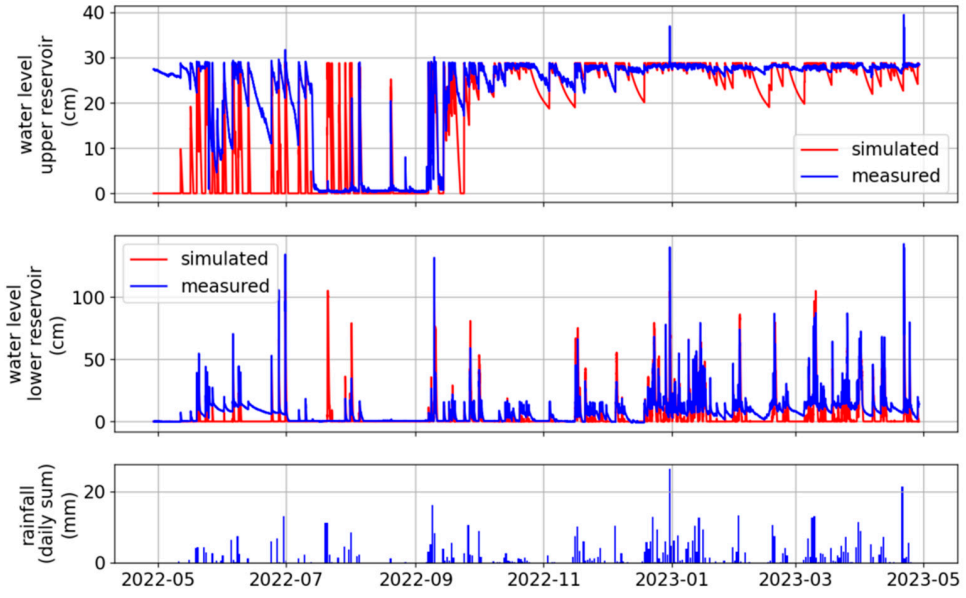

Figure 8. Comparison of model-predicted water levels with measured water levels during the second year of observation (29 April 2022–28 April 2023).

3.3. Retainable Heavy Rain Events

The retainable heavy rain events in relation to the volume of the reservoirs per area of connected impervious surface are shown in Figure 9. Compared to the period outside of the growing season, heavy rainfall can be retained with a higher return period in areas with prolonged rain durations during growing season. This can be explained by the fact that when there are lower rainfall levels, the influence of increased exfiltration through Perl

hoses intensifies during the growing season. With low to medium durations, retainability is mainly determined by the size of the reservoir. Furthermore, the retainability across the whole range of durations starts at a volume-to-area ratio of 200 m^3/ha. For reference, storm water retention tanks typically have a volume-to-area ratio of 100 to 300 m^3/ha in Germany. Full retainability starts at a ratio of 500 m^3/ha for heavy rain events with a return period of up to 100 years.

(**a**)

Duration	Return period								
	1 a	2 a	3 a	5 a	10 a	20 a	30 a	50 a	100 a
5 min	223.3	280.0	316.7	363.3	433.3	503.3	546.7	606.7	693.3
10 min	145.0	183.3	206.7	236.7	281.7	326.7	356.7	395.0	451.7
15 min	111.1	138.9	156.7	180.0	214.4	248.9	271.1	301.1	343.3
20 min	90.8	114.2	129.2	148.3	175.8	204.2	222.5	246.7	281.7
30 min	68.3	85.6	96.7	111.1	131.7	153.3	167.2	185.6	211.7
45 min	50.7	64.1	72.2	83.0	98.5	114.4	124.8	138.5	158.1
60 min	41.4	51.9	58.6	67.2	79.7	92.8	101.1	112.2	128.1
90 min	30.7	38.5	43.5	50.0	59.3	68.9	75.2	83.3	95.2
2 h	24.9	31.3	35.1	40.4	47.9	55.7	60.8	67.5	76.9
3 h	18.3	23.1	26.0	29.9	35.5	41.3	45.0	49.9	57.0
4 h	14.9	18.7	21.0	24.2	28.7	33.3	36.3	40.3	46.0
6 h	11.0	13.8	15.6	17.9	21.2	24.6	26.9	29.8	34.0
9 h	8.1	10.2	11.5	13.2	15.7	18.2	19.9	22.0	25.2
12 h	6.5	8.2	9.3	10.6	12.6	14.7	16.0	17.8	20.3
18 h	4.8	6.1	6.9	7.9	9.3	10.8	11.8	13.1	15.0
24 h	3.9	4.9	5.5	6.4	7.5	8.8	9.5	10.6	12.1
48 h	2.3	2.9	3.3	3.8	4.5	5.2	5.7	6.3	7.2
72 h	1.7	2.2	2.4	2.8	3.3	3.9	4.2	4.7	5.3
≥ 500 m^3/ha ≥ 400 m^3/ha ≥ 300 m^3/ha ≥ 200 m^3/ha ≥ 100 m^3/ha									

(**b**)

Duration	Return period								
	1 a	2 a	3 a	5 a	10 a	20 a	30 a	50 a	100 a
5 min	223.3	280.0	316.7	363.3	433.3	503.3	546.7	606.7	693.3
10 min	145.0	183.3	206.7	236.7	281.7	326.7	356.7	395.0	451.7
15 min	111.1	138.9	156.7	180.0	214.4	248.9	271.1	301.1	343.3
20 min	90.8	114.2	129.2	148.3	175.8	204.2	222.5	246.7	281.7
30 min	68.3	85.6	96.7	111.1	131.7	153.3	167.2	185.6	211.7
45 min	50.7	64.1	72.2	83	98.5	114.4	124.8	138.5	158.1
60 min	41.4	51.9	58.6	67.2	79.7	92.8	101.1	112.2	128.1
90 min	30.7	38.5	43.5	50.0	59.3	68.9	75.2	83.3	95.2
2 h	24.9	31.3	35.1	40.4	47.9	55.7	60.8	67.5	76.9
3 h	18.3	23.1	26.0	29.9	35.5	41.3	45.0	49.9	57.0
4 h	14.9	18.7	21.0	24.2	28.7	33.3	36.3	40.3	46.0
6 h	11.0	13.8	15.6	17.9	21.2	24.6	26.9	29.8	34.0
9 h	8.1	10.2	11.5	13.2	15.7	18.2	19.9	22.0	25.2
12 h	6.5	8.2	9.3	10.6	12.6	14.7	16.0	17.8	20.3
18 h	4.8	6.1	6.9	7.9	9.3	10.8	11.8	13.1	15.0
24 h	3.9	4.9	5.5	6.4	7.5	8.8	9.5	10.6	12.1
48 h	2.3	2.9	3.3	3.8	4.5	5.2	5.7	6.3	7.2
72 h	1.7	2.2	2.4	2.8	3.3	3.9	4.2	4.7	5.3
≥ 500 m^3/ha ≥ 400 m^3/ha ≥ 300 m^3/ha ≥ 200 m^3/ha ≥ 100 m^3/ha									

Figure 9. Retainable heavy rain events ($l \times (s \cdot ha)^{-1}$) in relation to the volume of the reservoirs per area of connected impervious surface during the growing season. The cross-hatched areas indicate events that could be retained, relative to the connected impervious surface, if the system was assumed to be empty but not if median water levels were assumed. (**a**) During the growing season ($h_{UR,med}$ = 0.412 cm and $h_{LR,med}$ = 14.54 cm); (**b**) outside of the growing season ($h_{UR,med}$ = 2.753 cm and $h_{LR,med}$ = 27.44 cm).

3.4. Drought Mitigation

According to the water distribution model, the irrigation reservoir is depleted in a mere 22 h during the growing season and in 40 days outside of the growing period. The infiltration reservoir is depleted in 22 h, unaffected by the time of year. In the measured data, the irrigation reservoir showed varying depletion rates, ranging from 22 h to 18 days during the growing season. Outside of the growing season, no depletion events were observed due to precipitation events refilling the reservoir before depletion could occur. The infiltration reservoir was usually depleted in around 22 h (excluding occurrences of potential backwater), which closely matches the model.

4. Discussion

4.1. Water Levels and Limits of the Model

The findings presented in Sections 3.1 and 3.2. show that a model using exfiltration and infiltration rates based on water levels and only using precipitation as an input value is limited in terms of its ability to correctly predict water levels in the system. The water levels in the transitional period from the non-growing season to the growing season, and vice versa, proved to be especially difficult to predict. However, the water levels outside of the growing season more closely matched the observed data. The soil water balance needs to be included in modelling approaches since it seems to be the most significant factor determining the exfiltration rates of Perl hoses. Further data obtained through subsequent years of study, i.e., analyzing the period when the roots reach the sphere of influence of the soil moisture content probes in Sys, are needed to determine the exact impact and expand the model with a factor accounting for soil moisture content.

4.2. Usage of Perl Hoses for Irrigation of Stormwater Tree Pits

Upon analysis of the measured water levels, a sort of self-regulating effect of the Perl hoses could be observed, where minimal exfiltration rates were observed outside of the growing season, while significantly higher rates were only observed during the growing season. A dependency of the soil water balance could not be observed because of the limitations of the experimental setup described in Sections 3.1 and 4.1.

4.3. Soil Moisture Content Probe Usage in Coarse-Grained Vegetation Substrates

During the study, a wide range of values of the soil moisture content under field capacity conditions could be observed. This could have been caused by two factors. Firstly, the soil moisture content probes were not calibrated to the specific vegetation substrate. The standard deviation of the measurements can be decreased from 3 Vol.-% to 1 Vol.-%. Secondly, the coarse-grained vegetation substrate prevents a uniform installation of the probes in the substrate, providing ununiform contact with the probes. This effect is not yet widely known, but workarounds, better probes, or different measurement systems will be needed since coarse-grained substrates, with their beneficial properties of a large REW range and high aeration, will likely see continued usage in stormwater tree pits.

4.4. Stormwater Tree Pits as Decentralized Storm Water Retention Tanks

Over the study period, a reduction of runoff by 90 to 92% could be observed, exceeding the runoff retention performance of bioretention systems of previous studies, which achieved runoff retention in the range of 50 to 70% [16–18].

The results of the simulation of heavy rain events show that the ALVEUS system performs akin to a decentralized storm water retention system, with the ability to retain heavy rain events, even when median water levels were assumed at the start, up to a return period of 10 years, offering a retention-volume-to-connected-impervious-area ratio of 300 m^3/ha, which matches the upper end of the ratio of decentralized storm water retention tanks in Germany [19].

4.5. Drought Mitigation

The results of this study show that, currently, no clear statement can be made about the drought mitigation effects of the ALVEUS system. Though the data show a clear increase in irrigation volume equal to 17 to 22 m^3 per year, since the roots likely have not reached the sphere of influence of the soil moisture content probes (see Section 4.1), the higher soil moisture content in the system cannot be solely accredited to the system working as intended. The system would be able to irrigate trees up to a height of 10 to 18 m [20]. The results show that the mitigation of drought periods can range from under a day to up to 18 days, depending on the exfiltration rate of the Perl hoses. Further data are required to determine with a degree of certainty that the Alveus stormwater tree pit system can adequately mitigate and reduce drought periods and thus decrease the need for external irrigation in the form of watering bags and water tankers.

5. Conclusions

In an increasingly urban society with increasing competition for land, alternatives to centralized and semi-centralized stormwater control measures must be developed. Our research shows that specialized storm water tree pits can retain heavy rain events with a return period of 10 years while matching the upper end of the retention-volume-to-connected-impervious-area ratio of 300 m^3/ha of decentralized storm water retention tanks. Simultaneously, the conditions of urban street trees can be improved by providing an additional irrigation volume of 17 to 22 m^3 per year. Perl hoses show promise as passive irrigation limiters, as exfiltration rates during the growing season are considerably higher than out of the growing season, though a link between the soil water balance and the exfiltration rates during the growing season could not be found due to limitations of root expansion in the study period. Further research will be needed once the root system has sufficiently developed to be monitored accordingly by the installed probes.

Supplementary Materials: The following supporting information can be downloaded at: https://www.mdpi.com/article/10.3390/w15162987/s1. Raw data files: water levels (Tables S1 and S2); soil moisture content (Tables S3 and S4); precipitation (Tables S5 and S6). Table S1: water levels—first year, Table S2: water levels—second year, Table S3: soil moisture content—first year, Table S4: soil moisture content—second year, Table S5: precipitation—first year, Table S6: precipitation—second year.

Author Contributions: Conceptualization, N.S. and H.G.; Data curation, N.S.; Formal analysis, N.S.; Funding acquisition, H.G.; Investigation, N.S.; Methodology, N.S.; Project administration, H.G.; Resources, N.S.; Software, N.S.; Supervision, H.G.; Validation, N.S. and H.G.; Visualization, N.S.; Writing—original draft, N.S. and H.G.; Writing—review and editing, N.S. and H.G. All authors have read and agreed to the published version of the manuscript.

Funding: This research was funded by the Federal Ministry for the Environment, Nature Conservation, Nuclear Safety and Consumer Protection (BMUV) based on a resolution of the German Bundestag (funding code: 67DAS196A).

Institutional Review Board Statement: Not applicable.

Informed Consent Statement: Not applicable.

Data Availability Statement: The data presented in this study are available in the article and the supplementary material.

Conflicts of Interest: The authors declare no conflict of interest.

References

1. Rahman, M.A.; Stratopoulos, L.M.F.; Moser-Reischl, A.; Zölch, T.; Häberle, K.H.; Rötzer, T.; Pretzsch, H.; Pauleit, S. Traits of trees for cooling urban heat islands: A meta-analysis. *Build. Environ.* **2020**, *170*, 106606. [CrossRef]
2. Mullaney, J.; Lucke, T.; Trueman, S.J. A review of benefits and challenges in growing street trees in paved urban environments. *Landsc. Urban Plan.* **2015**, *134*, 157–166. [CrossRef]
3. Kluge, B.; Pallasch, M.; Geisler, D.; Hübner, S. Straßenbäume und dezentrale Versickerung als Beitrag wassersensibler Stadtentwicklung—Teil 1. *KA Korresp. Abwasser Abfall* **2022**, *69*, 358–376. [CrossRef]

4. Grey, V.; Livesley, S.J.; Fletcher, T.D.; Szota, C. Establishing Street trees in stormwater control measures can double tree growth when extended waterlogging is avoided. *Landsc. Urban Plan.* **2018**, *178*, 122–129. [CrossRef]
5. Bartens, J.; Day, S.D.; Harris, J.R.; Wynn, T.M.; Dove, J.E. Transpiration and root development of urban trees in structural soil stormwater reservoirs. *Environ. Manag.* **2009**, *44*, 646–657. [CrossRef] [PubMed]
6. Xiao, Q.; McPherson, E.G. Performance of engineered soil and trees in a parking lot bioswale. *Urban Water J.* **2011**, *8*, 241–253. [CrossRef]
7. Scharenbroch, B.C.; Morgenroth, J.; Maule, B. Tree Species Suitability to Bioswales and Impact on the Urban Water Budget. *J. Environ. Qual.* **2016**, *45*, 199–206. [CrossRef] [PubMed]
8. Denman, L.; May, P.B.; Breen, P.F. An investigation of the potential to use street trees and their root zone soils to remove nitrogen from urban stormwater. *Australas. J. Water Resour.* **2006**, *10*, 303–311. [CrossRef]
9. Climate-Data.org. Available online: https://de.climate-data.org/europa/deutschland/nordrhein-westfalen/coesfeld-890044/ (accessed on 15 June 2023).
10. Granier, A.; Reichstein, M.; Bréda, N.; Janssens, I.A.; Falge, E.; Ciais, P.; Grünwald, T.; Aubinet, M.; Berbigier, P.; Bernhofer, C.; et al. Evidence for soil water control on carbon and water dynamics in European forests during the extremely dry year: 2003. *Agric. For. Meteorol.* **2007**, *143*, 123–145. [CrossRef]
11. dwd.de. Raster der Wiederkehrintervalle für Starkregen (Bemessungsniederschläge) in Deutschland (KOSTRA-DWD), Version 2020. Available online: https://www.dwd.de/DE/leistungen/kostra_dwd_rasterwerte/kostra_dwd_rasterwerte.html (accessed on 23 May 2023).
12. dwd.de. Available online: https://www.dwd.de/DE/service/lexikon/Functions/glossar.html?lv2=102868&lv3=102890 (accessed on 3 June 2023).
13. Granier, A.; Bréda, N.; Biron, P.; Villette, S. A lumped water balance model to evaluate duration and intensity of drought constraints in forest stands. *Ecol. Model.* **1999**, *116*, 269–283. [CrossRef]
14. Black, T.A. Evapotranspiration from Douglas fir stands exposed to soil water deficits. *Water Resour. Res.* **1979**, *15*, 164–170. [CrossRef]
15. Dunin, F.X.; Aston, A.R. The development and proving of models of large scale evapotranspiration: An Australian study. *Agric. Water Manag.* **1984**, *8*, 305–323. [CrossRef]
16. Hunt, W.F.; Jarrett, A.R.; Smith, J.T.; Sharkey, L.J. Evaluating bioretention hydrology and nutrient removal at three field sites in North Carolina. *J. Irrig. Drain. Eng* **2006**, *132*, 600–608. [CrossRef]
17. Li, H.; Sharkey, L.J.; Hunt, W.F.; Davis, A.P. Mitigation of impervious surface hydrology using bioretention in North Carolina and Maryland. *J. Hydrol. Eng.* **2009**, *14*, 407–415. [CrossRef]
18. Page, J.L.; Winston, R.J.; Mayes, D.B.; Perrin, C.; Hunt, W.F. Retrofitting with innovative stormwater control measures: Hydrologic mitigation of impervious cover in the municipal right-of-way. *J. Hydrol.* **2015**, *527*, 923–932. [CrossRef]
19. Deutsche Vereinigung für Wasserwirtschaft, Abwasser und Abfall e.V. *DWA-A 117 Bemessung von Regenrückhalteräumen*; Deutsche Vereinigung für Wasserwirtschaft, Abwasser und Abfall e.V.: Hennef, Germany, 2013.
20. BlueGreenStreets. BlueGreenStreets als Multicodierte Strategie zur Klimafolgenanpassung—Wissenstand 2020, April 2020, Hamburg. Statusbericht im Rahmen der BMBF-Fördermaßnahme, Ressourceneffiziente Stadtquartiere für die Zukunft (RES:Z). Available online: https://repos.hcu-hamburg.de/handle/hcu/522 (accessed on 5 June 2023).